Received 1 February 2022
Revised 20 March 2022
Accepted 27 April 2022

Experimental study of the wheel/rail impact caused by wheel flat within 400 km/h using full-scale roller rig

Chongyi Chang, Yuanwu Cai and Bo Chen
Railway Science and Technology Research and Development Center, China Academy of Railway Sciences Corporation Limited, Beijing, China
Qiuze Li
National Engineering Research Center of Railway Vehicles, CRRC Changchun Railway Vehicles Corporation Limited, Changchun, China, and
Pengfei Lin
National Engineering Research Center of Railway Vehicles, CRRC Qingdao Sifang Rolling Stock Research Institute Co Ltd, Qingdao, China

Abstract

Purpose – In service, the periodic clashes of wheel flat against the rail result in large wheel/rail impact force and high-frequency vibration, leading to severe damage on the wheelset, rail and track structure. This study aims to analyze characteristics and dynamic impact law of wheel and rail caused by wheel flat of high-speed trains.

Design/methodology/approach – A full-scale high-speed wheel/rail interface test rig was used for the test of the dynamic impact of wheel/rail caused by wheel flat of *high-speed* train. With wheel flats of different lengths, widths and depths manually set around the rolling circle of the wheel tread, and wheel/rail dynamic impact tests to the flats in the speed range of 0–400 km/h on the rig were conducted.

Findings – As the speed goes up, the flat induced the maximum of the wheel/rail dynamic impact force increases rapidly before it reaches its limit at the speed of around 35 km/h. It then goes down gradually as the speed continues to grow. The impact of flat wheel on rail leads to 100–500 Hz middle-frequency vibration, and around 2,000 Hz and 6,000 Hz high-frequency vibration. In case of any wheel flat found during operation, the train speed shall be controlled according to the status of the flat and avoid the running speed of 20 km/h–80 km/h as much as possible.

Originality/value – The research can provide a new method to obtain the dynamic impact of wheel/rail caused by wheel flat by a full-scale high-speed wheel/rail interface test rig. The relations among the flat size, the running speed and the dynamic impact are hopefully of reference to the building of speed limits for HSR wheel flat of different degrees.

Keywords Wheel/rail impact force, High-frequency vibration, Maintenance rules, Speed limit

Paper type Research paper

This study has been subsidized by CHINA RAILWAY Scientific and Technological Research and Development Project (contract no. 2015J007-E and 2016J007-H), to which the authors hereby express their appreciation.

1. Introduction

Wheel flat, a common tread defect, is largely caused by repeated wheel/rail abrasion amid the braking and the rolling of wheels over a long period of time. In service, the periodic clashes of wheel flat against the rail result in large wheel/rail impact force and high-frequency vibration, leading to severe damage on the wheelset, rail and track structure. It needs to be noted that the difference in wheel flat undermines operational safety and riding comfort to different extents, and at the same time, it significantly intensifies the noise induced and piles on maintenance costs.

In the past decades, the studies of the wheel/rail dynamic impact forces and the damages which the flat causes mainly reply on numerical analysis (Bogdevicius, Zygiene, Bureika, & Dailydka, 2016; Pieringer, Kropp, & Nielsen, 2014; Uzzal, Ahmed, & Bhat, 2013; Steenbergen, 2007; Ren, 2019; Han, Jing, & Liu, 2017) and experimental means (Jergeus *et al.*, 1999; Sandstr and Ekberg, 2009). For the sake of operation safety (Technical Specialist Rolling Stock Performance Standards, 2013; Railway Wheelsets, 2010), three limits are to be imposed in the relevant regulations for the maintenance of wheel flat, namely the size of wheel flat, running speed and the impact load.

Ren (2019) set up both a 3D model for flatted wheel and a vehicle/rail coupling dynamics model. With wheel rotation and wheel/rail contact geometry employed, the studies found that both the length and the width of the flat affected the wheel/rail system dynamics impact. The result of the study shows: when the width of wheel flat was 41.7 mm and the running speed increased with the range of 100 km/h to 220 km/h, the wheel/rail vertical force went up, which then went down as the speed continues to increase.

Han *et al.* (2017) established a 3D finite element model for wheel/rail rolling contact using LS-DYNA 3D/explicit code. The influences of train speed, flat length and a 17 *t* axle load on the vertical wheel/rail impact response were studied respectively. The result shows that the maximum value for the vertical impact force changes in a non-monotonic way with the variation of train speed. In case where the flat length is 60 mm, the maximum value climbed up with the speed increase to a peak value of 325 kN before the speed reaches 150 km/h, and it went down slowly as the speed accelerated to 350 km/h.

For the sake of operation safety, the existing rules (Rules for Operation and Maintenance of Railway EMUs, 2017) on wheel flat tolerance for Chinese EMU stipulate that the length and the depth of the flat are not to exceed 25 mm and 0.25 mm, respectively, when the wheel diameter is less 840 mm; otherwise, the length and the depth are not to go beyond 30 mm and 0.25 mm, respectively. That aside, different flats are subject to different speed restrictions. For example, when the depth is 0.25 mm to 0.5 mm, the operation speed shall not exceed 200 km/h; when the depth falls between 0.5 mm and 1 mm, the speed shall not exceed 120 km/h. Therefore, in the development of the rules for the wheel flat tolerance of *high-speed* trains, the relations among the flat size, the running speed and the dynamic impact must be fully considered, which in turn gives rise to the necessities of relevant studies into this matter.

Till today, simulation-dynamic studies and transient finite element modeling represents the extensively used approach when it comes to the relation between wheel flat and the vibration of wheel/rail system. Given the complexity of the rolling contact and the unsatisfying accuracy of numerical simulation, it is difficult to obtain good results. In comparison, damage to the wheel/rail system tends to be the sure results for a field test of wheel flat, which is particularly true when it comes to high-speed test. This also explains the rarity of a field test for this matter.

In this paper, wheel flats of different lengths and depths around the tread are set manually, and a full-scale high-speed wheel/rail interface test rig is used to study the dynamic impact of wheel and rail caused by wheel flat of high-speed trains.

2. High-speed wheel/rail interface test rig

The test rig applied, a full-scale high-speed wheel/rail interface test rig, is a technically advanced facility in the ownership of China Academy of Railway Sciences Corporation Limited (CARS). With perfect measuring and testing functions as well as a maximum testing speed of 500 km/h, it can facilitate both fundamental and forward-looking studies, and provide what it takes for a simulated integrated test of wheel/rail products for design and reliability improvement, contributing significantly to the experimental and theoretical studies of high-speed wheel/rail interface.

The test rig consists of rail-wheel system, wheelset system, hydraulic excitation system, environment simulation system for track contact interface, numerically controlled rail/wheel profile lathing device, high-pressure hydraulic supply unit, lubrication unit, calibrator, electrical equipment, measurement and data acquisition system, as well as control system, etc. In Figure 1, the test rig's outfit for impact test is shown, and the key technical parameters are seen in reference (Chang, Chen, Cai & Wang, 2019). Capable of simulating dry, wet and oily environment for wheel/rail interface, the test rig can measure a range of parameters, including the rotation speed of wheelset (adhesion wheel), that of track wheel, wheel/rail contact force, wheelset lateral displacement, wheelset attack angle, hydraulic excitation force, motor torque and braking torque. It can be used to carry out tests of high-speed wheel/rail adhesion, creep, derailment, wear, fatigue, braking, noise, dynamic calibration of instrumented wheelsets, as well as the matching and optimization of wheel/rail geometry and material properties.

3. Test methods of wheel flat impact using high-speed wheel/rail test rig

3.1 Prefabrication of wheel flat

The dimensions applied for the prefabrication of the flat wheel is seen in reference (Uzzal *et al.*, 2013), in which the depth d_p is calculated with the flat length l and the nominal rolling radius r_w of the wheel, which is determined by Equation (1). The flat width d_w is determined by the flat depth d_p, and the rail head radius r_r at the wheel/rail contact point, which is determined by Equation (2). Table 1 shows the sizes of the flat left on new LM_A wheel as it runs on TB60 rail, in which the nominal rolling radius r_w is 460 mm, and the rail head radius r_r is 300 mm. Table 1 is used for the prefabrication of the flat (see Figure 2 for the photos).

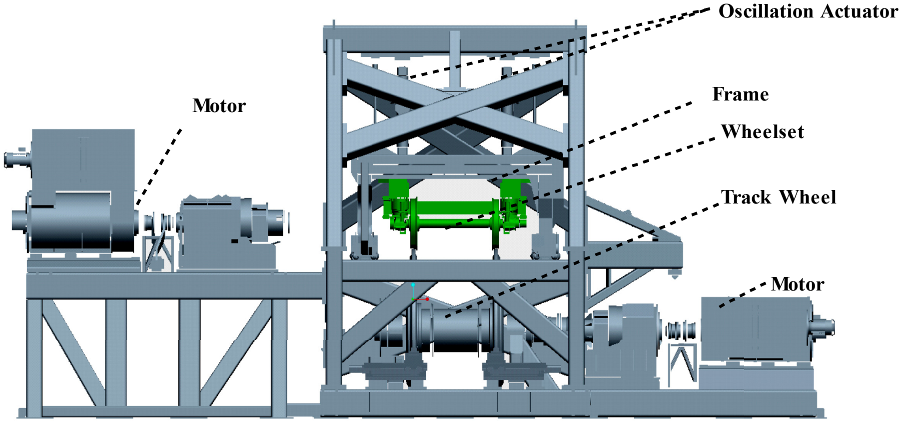

Figure 1.
Test rig's outfit for impact test of wheel flat

$$d_p = r_w\left[1-\cos\left(\frac{l}{2r_w}\right)\right] \tag{1}$$

$$d_w = 2\sqrt{r_r-(r_r-d_p)^2} \tag{2}$$

3.2 Measurement method of wheel/rail impact force and vibrational acceleration

The wheel/rail vertical forces are measured by the strain gauges installed on the circular section of the axle where the radius is 75 mm and the sampling frequency is set at 2,000 Hz.

Item	Depth (mm)	Length (mm)	Width (mm)
1	0.24	30	24.2
2	0.43	40	32.3
3	0.68	50	40.4
4	0.98	60	48.4
5	1.33	70	56.5

Table 1. Length, width and depth of five types of wheel flats

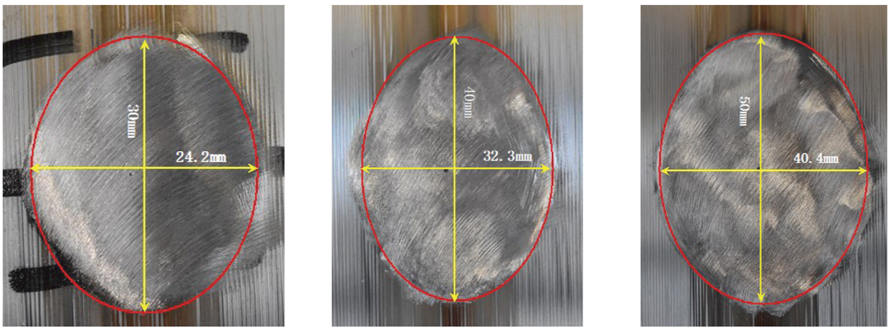

Length 30mm, Width 24.2mm
(a)
Length 40mm, Width 32.3mm
(b)
Length 50mm, Width 40.4mm
(c)

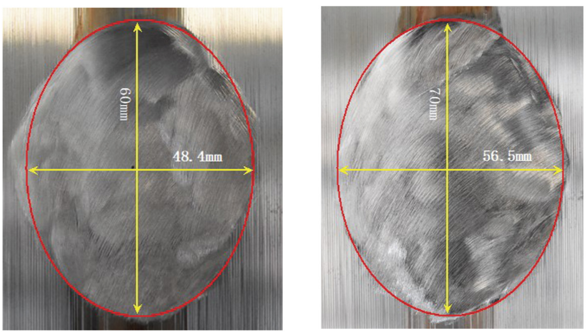

Length 60mm, Width 48.4mm
(d)
Length 70mm, Width 56.5mm
(e)

Figure 2. Wheel flat size

The vibrational accelerations of wheel rail dynamic impact are measured by the acceleration sensors installed at the end of the axle box with the sampling frequency being 12,800 Hz.

3.3 Test program

(1) The surface of the wheelset and the track wheel shall be cleaned with alcohol or acetone before the test to remove any possible stain and to keep the rolling surface clean and dry.

(2) A wheel flat is to be prefabricated on one wheel of the wheelset.

(3) Impose a wheel/rail vertical load of 150 kN (equivalent to an axle load of 15 t) via a vertical actuator while the lateral displacement and yaw angle of the wheelset are to be kept at 0 by a lateral and two yaw angle actuators.

(4) Start the drive motor to rotate the track wheel, which in turn initiates the rotation of the wheelset under the wheel/rail friction. As the contact point of the track wheel and the wheelset reaches the specified speed, keep the speed for one minute.

(5) Record the wheel/rail vertical force and the vibrational acceleration of wheel/rail impact.

4. Analysis of testing results

4.1 Wheel/rail impact dynamics

In case where the wheel flat reaches 0.43 mm, 40 mm and 32.3 mm in depth, length and width, respectively, the test speed for wheel/rail impact dynamics is set at 40 km/h. The wheel/rail vertical force in time domain is shown in Figure 3. The wheel/rail impacts are depicted in the figures for two cycles. It can be noticed that before the flat, the wheel/rail vertical force is kept at 75 kN. However, as the rail takes a toll from the flat, the maximum vertical impact force tops at 133 kN, recording a 77% increase. And the very short duration of the wheel/rail impact brings about high-frequency vibration.

The vertical impact vibration acceleration of the axle box in time domain is shown in Figure 4, in which the maximal vertical impact vibration acceleration is 913 m/s^2. Figure 5 shows the results of the time frequency analysis of wheel/rail dynamic impact vibration acceleration, with not only 100–500 Hz middle-frequency vibration, but also about 1,300 Hz and 4,800 Hz high-frequency vibration. Figure 6 displays the attenuation trend of vibration acceleration of wheel/rail dynamic impact where it takes 0.05 s for the vertical acceleration to decay exponentially by 90% from its peak value. The attenuation of the vibration acceleration amplitude can be described as follows.

$$a_A = 4.918/(t - 0.05971) \tag{3}$$

For the abrasion, the test results of wheel/rail dynamics impact are analyzed at the speed of 400 km/h. The wheel/rail vertical force in time domain is shown in Figure 7. The test results show that the maximum vertical impact force is 82 kN, which is only 9% larger than the wheel weight. The vertical impact vibration acceleration of the axle box in time domain is shown in Figure 8, in which the maximum vertical impact vibration acceleration is 220 m/s^2. The impact feature is not obvious in Figures 7 and 8. Time frequency analysis of wheel/rail dynamic impact vibration acceleration is shown in Figure 9, which shows there are 250–500 Hz middle-frequency vibration and 1800 Hz high-frequency vibration characteristic.

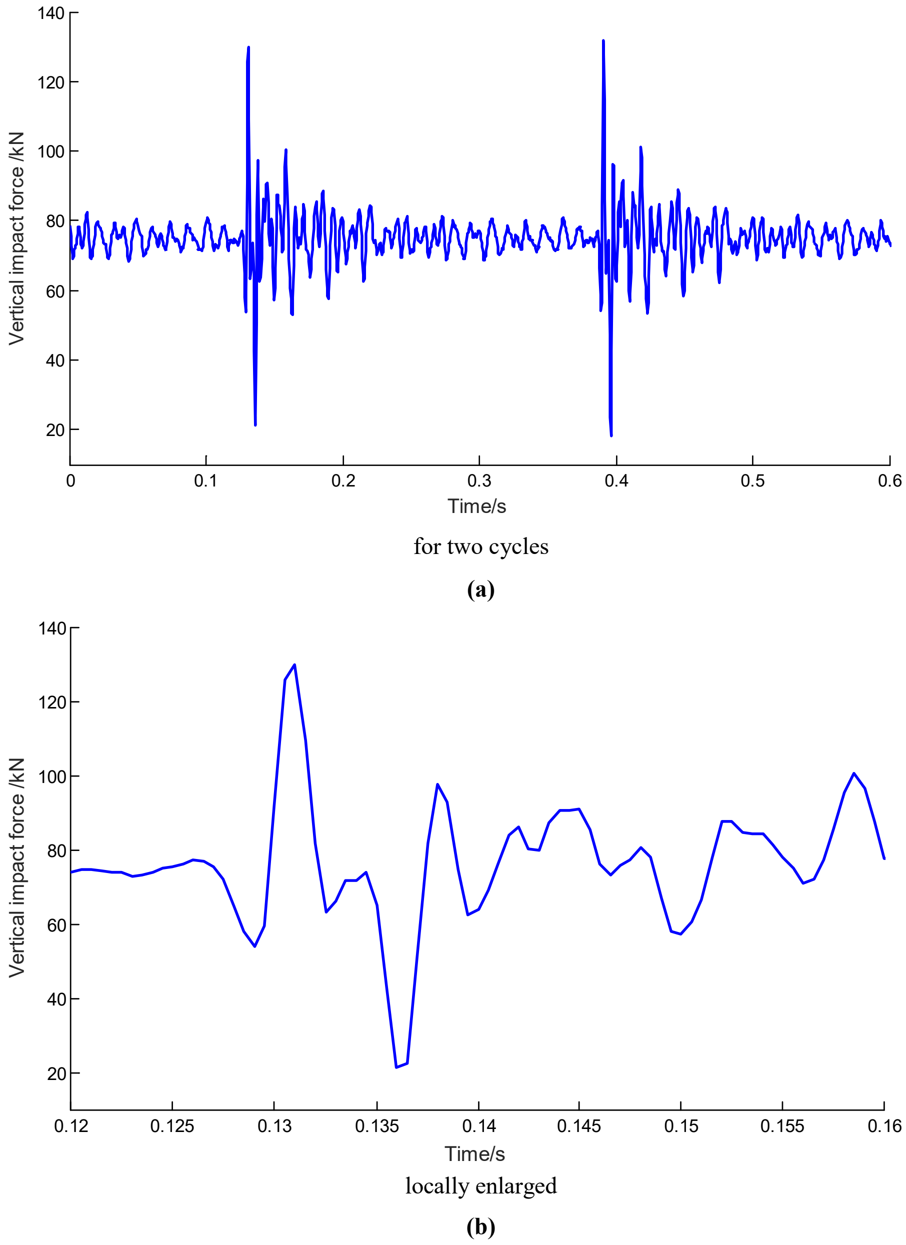

Figure 3.
Wheel/rail dynamic impact force at 40 km/h

4.2 Effect of speed on wheel/rail impact dynamics

Figure 10 depicts the relation between running speed and wheel/rail impact dynamics in case where the flat records 0.43 mm, 40 mm and 32.3 mm in depth, length and width, respectively. It can be seen that the maximum of the impact force increases dramatically as the speed rises

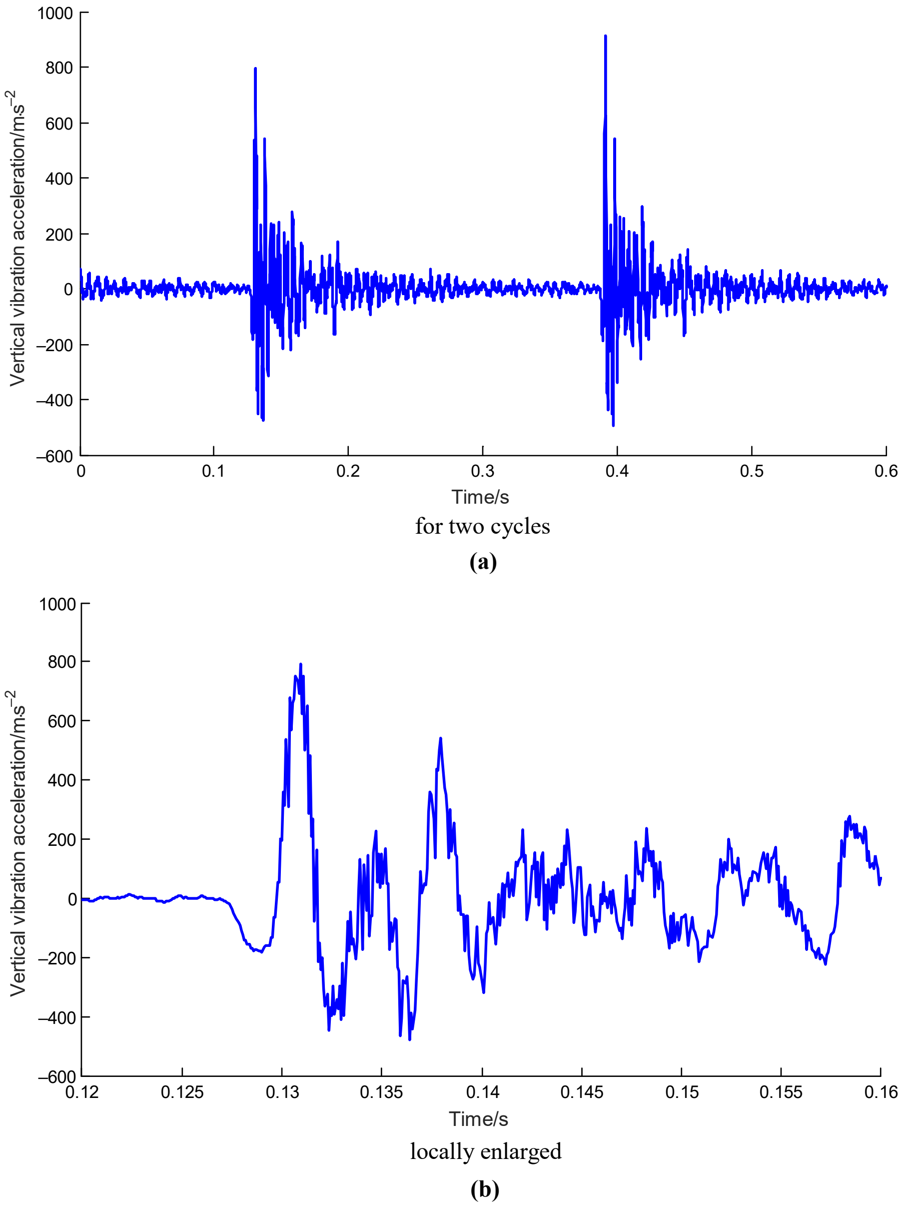

Figure 4.
Vibration acceleration of wheel/rail dynamic impact at 40 km/h

from 0 to 35 km/h and then plummets from 35 km/h to 200 km/h, after which it decreases slowly from 200 km/h to 400 km/h. To put things in perspective, the maximum of the wheel/rail impact force of 135 kN at 35 km/h represents a 80% increase on the wheel weight of 75 kN and a 38% decrease from the 84 kN at 400 km/h.

Figure 11 shows the development of the maximum of the vibration acceleration of wheel/rail vertical impact with the change of test speed. The results show that as the speed goes up,

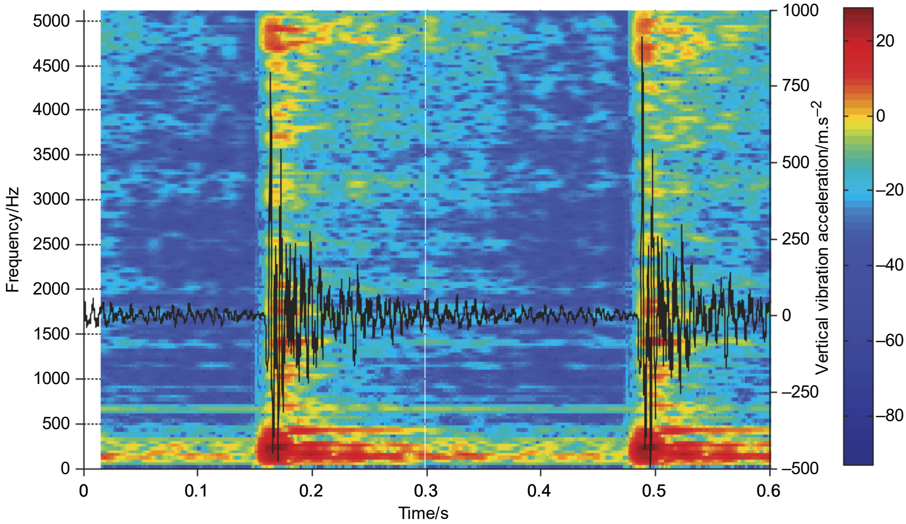

Figure 5.
Time frequency analysis of vibration acceleration of wheel/rail dynamic impact at 40 km/h

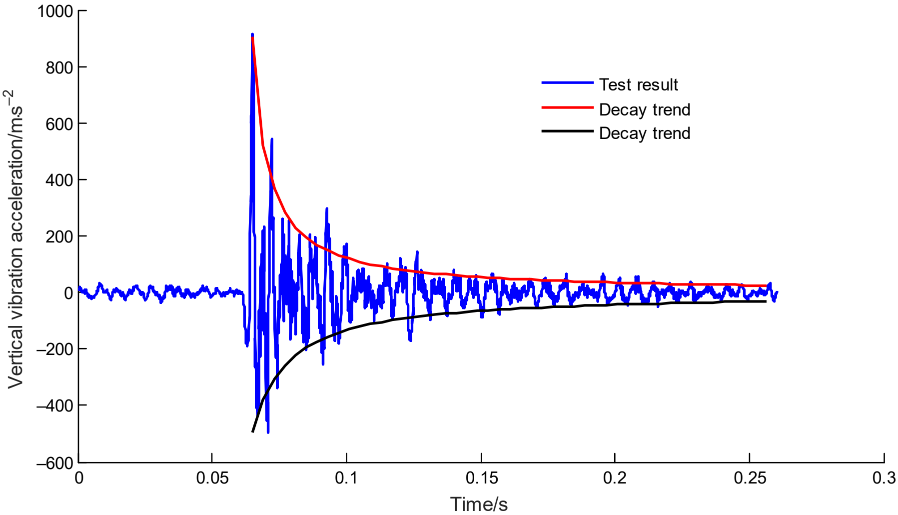

Figure 6.
Attenuation of vibration acceleration of wheel/rail dynamic impact

the maximum of the axle box vibration acceleration increases and reaches a limit of 913 m/s^2 near 35 km/h, and then declines gradually to 233 m/s^2 at 250 km/h. Within the speed range from 250 km/h to 400 km/h, the maximum of the impact vibration acceleration increases only slightly as the vibration of the wheel/rail system itself intensifies with the increase of speed.

4.3 Effect of flat size on wheel/rail impact dynamics

Figure 12 displays the relations between the maximum of the wheel/rail dynamic impact and flat dimension. It can be seen that the maximum of the impact forces all increase first as the speed goes up, and then reaches the top at about 35 km/h. The curves go down afterward as

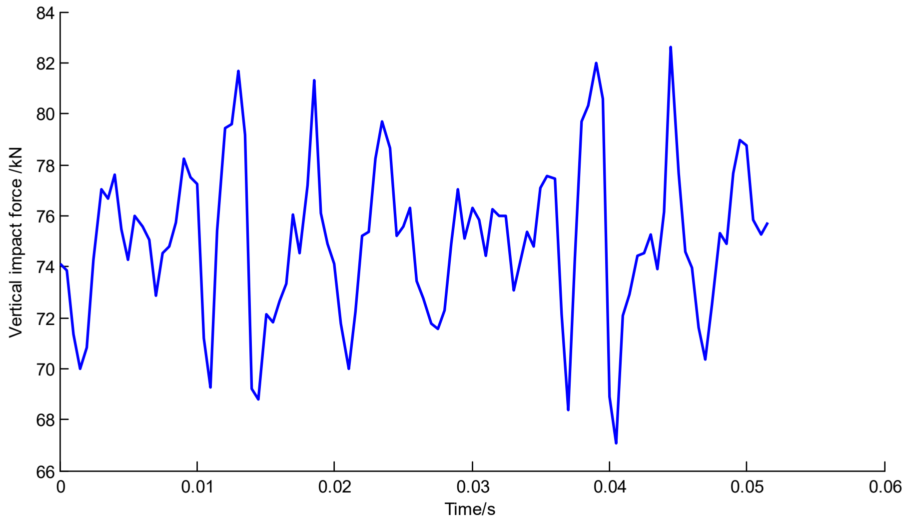

Figure 7.
Wheel/rail dynamic impact force at 400 km/h

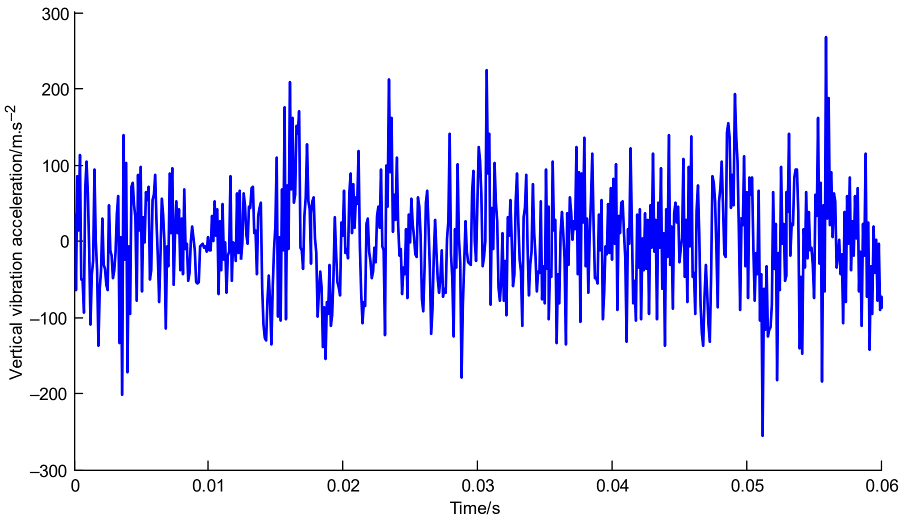

Figure 8.
Vibration acceleration of wheel/rail dynamic impact at 400 km/h

the speed continues to climb up. At the same speed level, the increase in flat size translates into higher impact forces. For flat with length less than 50 mm, the maximum of impact force induced does not go beyond 165 kN (EN 14363, 2016; UIC 518, 2009), while for that of 60 mm in length and 0.98 mm in depth, the maximum of the impact force declines by about 51% from 178 kN at 35 km/h to 88 kN at 400 km/h. For the flat of 1.33 mm in depth and 70 mm in length, the maximum impact force registers an around 55% decrease from 201 kN at 35 km/h to 90 kN at 400 km/h and is even more than twice the static load in the speed range of 24.3 km/h–71.4 km/h.

The relation of the maximum of the wheel/rail vertical impact vibration acceleration versus the speed is shown in Figure 13. As shown in Figure 13, the maximum of the axle box

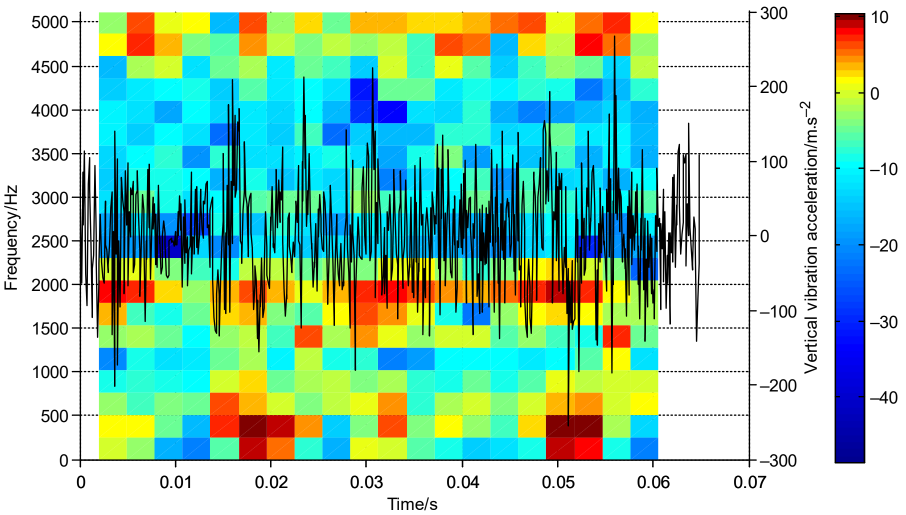

Figure 9.
Time frequency analysis of vibration acceleration of wheel/rail dynamic impact at 400 km/h

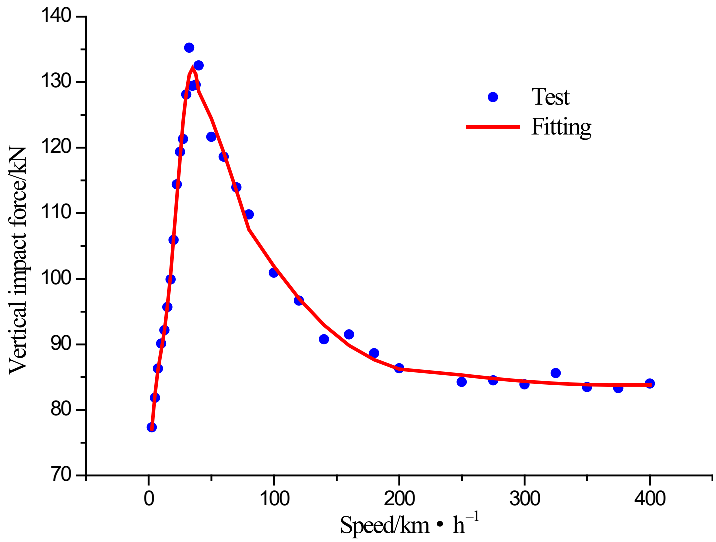

Figure 10.
Relations between the maximum of the wheel/rail dynamic impact force and the speed

vibration acceleration increases amid the speed-up process and reaches its limit before it decreases with the continuous speed increase. At 250 km/h, the development of the curves start to vary as that with over 60 mm long flat go down and that with less than 60 mm-long flat head upward. It needs to be pointed out that the maximum of the vertical acceleration at the same speed goes up with the increase of the flat size. For the flat with depth of 0.98 mm and length of 60 mm, the maximum of the impact vibration acceleration decreases from 2,045 m/s^2 at 37.5 km/h to 380 m/s^2 at 400 km/h, down by 81%, while for that 1.33 mm deep and 70 mm long, the maximum of the acceleration declines from 2,095 m/s^2 at 37.5 km/h to 398 m/s^2 at 400 km/h, down by 81%.

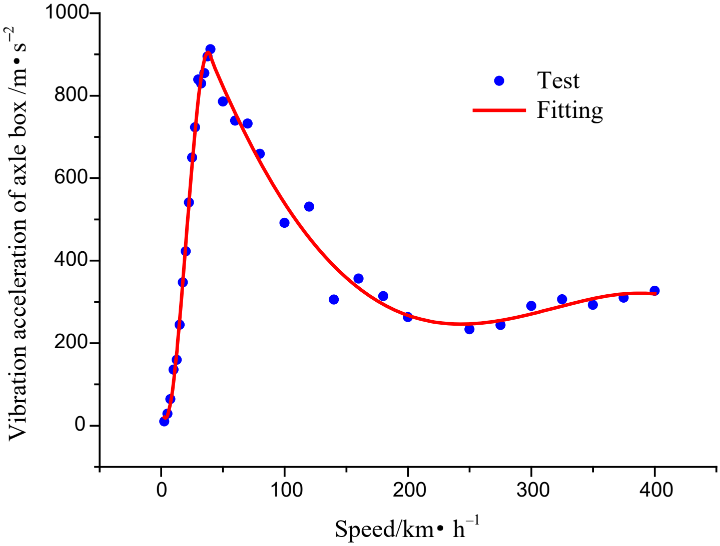

Figure 11.
Relations between the maximum of the vibration acceleration of wheel/rail dynamic impact and the speed

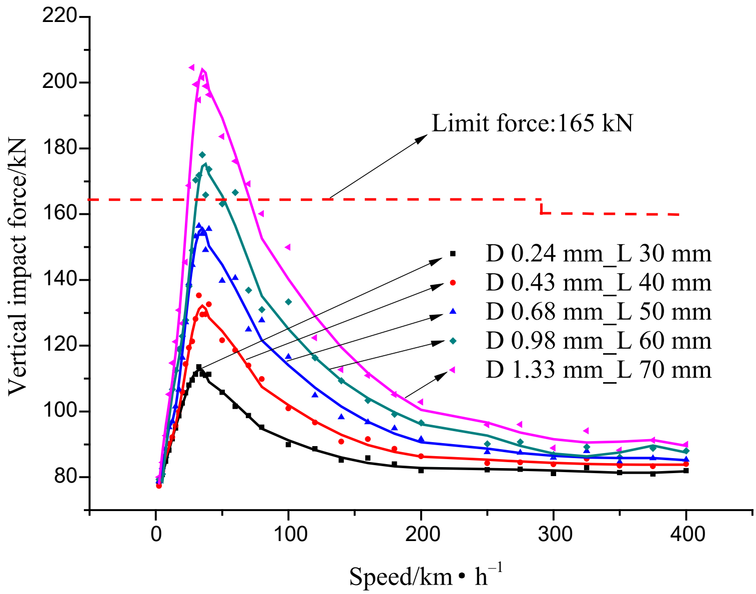

Figure 12.
Relations between the speed and the maximum of wheel/rail dynamic impact force induced by flats of different sizes

4.4 Analysis of impact force safety map of flat size and speed

See Figure 14 for the distribution diagram of the wheel flat impact force drawn in reference to Figure 12. It can be seen in Figure 14 that red, a tongue-shaped distribution, represents the danger zone, meaning the maximum of the impact force has exceeds the 165 kN; yellow, the transition zone, means the value falls between 150 and 165 kN; green and blue, the safe zone, mean the value is less than 150 kN. In case of any wheel flat noticed during EMU operation, the speed shall be properly controlled according to the status of the flat to ensure that does not

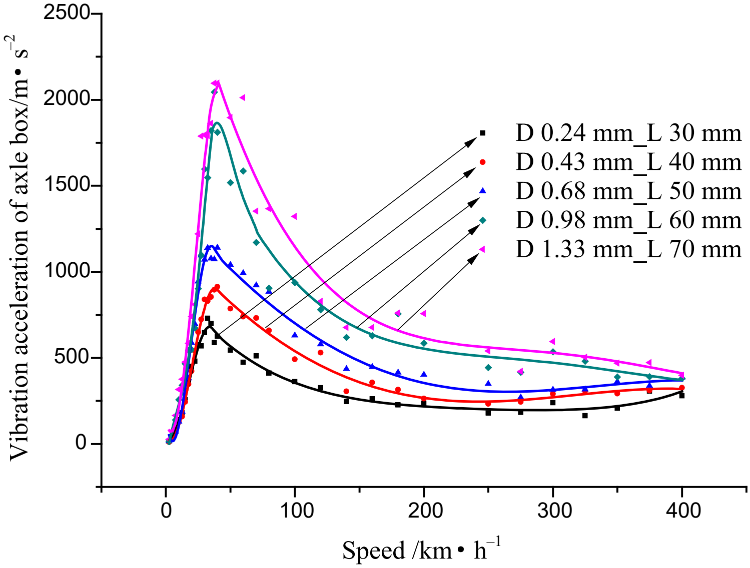

Figure 13.
Relations between the speed and the maximum of the vibration acceleration of wheel/rail dynamic impact induced by flats of different sizes

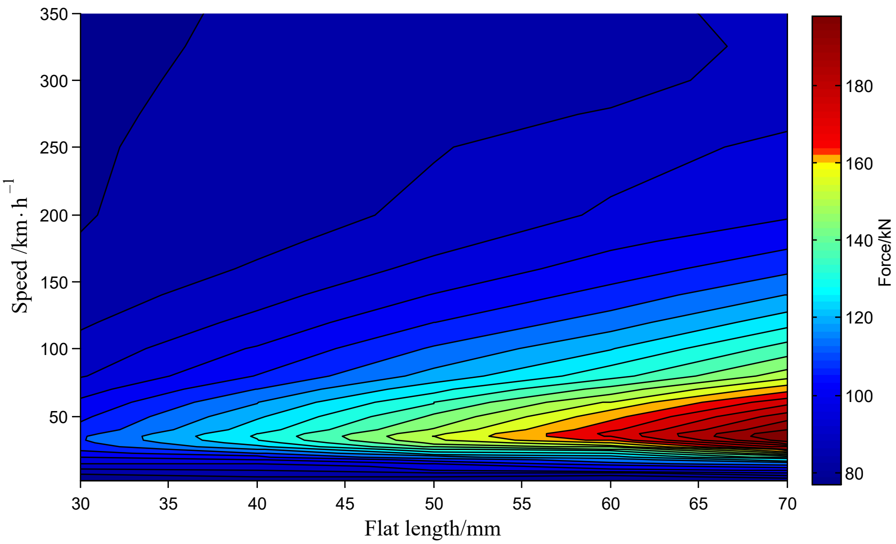

Figure 14.
Safety margin of flat depth and speed

go below a certain speed level or below 20 km/h. When the flat length is more than 60 mm, the operation is recommended to halt with immediate treatment needed at once.

5. Conclusions

(1) The impact of flat wheel on rail leads to both 100–500 Hz middle-frequency vibration and around 2,000 Hz and 6,000 Hz high-frequency vibration. Shortly after the wheel flat impact, the impact force and the vibration acceleration plummet rapidly.

(2) As the speed goes up, the flat induced the maximum of the wheel/rail dynamic impact force increases rapidly before it reaches its limit at the speed level of around 35 km/h. It then goes down gradually as the speed continues to grow. As the speed climbs up within the range of 35 km/h–200 km/h, the maximum value of impact force decreases rapidly, however, as the speed rises within 200 km/h–400 km/h, the value slowly decreases.

(3) The increase of flat dimension results in the increase of the maximum of the wheel/rail impact force. For a 60 mm long flat, the maximum of the impact force induced at 31.4~50.7 km/h is larger, even more than twice the static load.

(4) It can be concluded from the safety margin diagram that the danger zone takes the shape of a tongue, and major wheel/rail impact is prone to take place at low-medium speed levels. In case of any wheel flat found during operation, the train speed shall be controlled according to the status of the flat and avoid the running speed of 20 km/h–80 km/h as much as possible. In case where the flat exceeds 60 mm in length, the train shall be taken out of service for immediate treatment.

References

Bogdevicius, M., Zygiene, R., Bureika, G., & Dailydka, S. (2016). An analytical mathematical method for calculation of the dynamic wheel-rail impact force caused by wheel flat. *Vehicle System Dynamics*, *54*(5), 689–705.

Chang, C., Chen, B., Cai, Y., & Wang, J. (2019). An experimental study of high speed wheel-rail adhesion characteristics in wet condition on full scale roller rig. *Wear*, 440–441.

Han, L., Jing, L., & Liu, K. (2017). An investigation on wheel/rail impact dynamics with a three-dimensional flat model. *Journal of Modern Transportation*, *25*(2), 124–131.

Jergeus, J., Odenmarck, C., Lunden, R., Sotkovszki, P., Karlsson, B., & Gullers, P. (1999). Full-scale railway wheel flat experiments. *Proceedings of the Institution Mechanical Engineers*. Part F, Journal of Rail and Rapid Transit, *213*, 1-13.

Pieringer, A., Kropp, W., & Nielsen, J. (2014). The influence of contact modelling on simulated wheel/rail interaction due to wheel flats. *Wear*, *314*, 273–281.

Railway applications - Testing and Simulation for the acceptance of running characteristics of railway vehicles - Running Behaviour and stationary tests (2016). *EN 14363*. CEN-CENELEC Management Centre.

Railway Wheelsets (2010). *Railway Group Standard GM/RT2466*. Rail Safety and Standards Board Evergreen House.

Ren, Z. (2019). An investigation on wheel/rail impact dynamics with a three-dimensional flat model. *Vehicle System Dynamics*, *57*(3), 369–388.

Rules for Opration and Maintenance of Railway EMUs (2017). *Railway general transportation*. China Railway Publish Hours.

Sandstr, J., & Ekberg, A. (2009). Predicting crack growth and risks of rail breaks due to wheel flat impacts in heavy haul operations. *Proceedings of the Institution of Mechanical Engineers, Part F: Journal of Rail and Rapid Transit*, *223*, 153–161.

Steenbergen, M. (2007). The role of the contact geometry in wheel/rail impact due to wheel flats. *Vehicle System Dynamics*, *45*(12), 1097–1116.

Technical Specialist Rolling Stock Performance Standards (2013). *Engineering standard rolling stock. ESR 0330*. Wheel Defect Manual. Version 1.2.

Testing and approval of railway vehicles from the point of view of their dynamic behaviour-safety – track fatigue-ride quality (2009). *UIC Code 518*. Paris: International Union of Railways.

Uzzal, R., Ahmed, A., & Bhat, R. (2013). Modelling, validation and analysis of a three-dimensional railway vehicle-track system model with linear and nonlinear track properties in the presence of wheel flats. *Vehicle System Dynamics*, *51*(11), 1695–1721.

Corresponding author
Chongyi Chang can be contacted at: chychang@163.com